Materials Today Chemistry 21 (2021) 100491

Contents lists available at ScienceDirect

Materials Today Chemistry

journal homepage: www.journals.elsevier.com/materials-today-chemistry/

Photochromic polyoxometalate–based enzyme-free reusable sensors for real-time colorimetric detection of alcohol in sweat and saliva

M. Sánchez [a], A. González [a], L. Sabio [a], W. Zou [b], R. Ramanathan [b], V. Bansal [b, *], J.M. Dominguez-Vera [a, **]

[a] Departamento de Química Inorgánica and Instituto de Biotecnología, Universidad de Granada, Granada, 18071, Spain
[b] Ian Potter NanoBioSensing Facility, NanoBiotechnology Research Laboratory, School of Science, RMIT University, Melbourne, Victoria, 3000, Australia

ARTICLE INFO

Article history:
Received 24 February 2021
Received in revised form
30 April 2021
Accepted 1 May 2021
Available online xxx

Keywords:
Phosphotungstic acid
Ethanol sensing
Colorimetric sensors
Mobile phone

ABSTRACT

This study describes a new strategy for real-time detection of alcohol in saliva and sweat. Phosphotungstic acid (PTA) is a colorless, photoelectrochromic heteropoly acid that can be reduced by ethanol under ultraviolet (UV) radiation to produce an intense blue color. This system has useful properties in the development of a new alcohol sensor: (1) the blue color can be detected by the naked eye or mobile camera, even at low ethanol concentrations; (2) color intensity is proportional to ethanol concentration; and (3) once exposed to air, reduced PTA is subsequently oxidized and returns to its colorless state offering sensor reusability. Based on these properties, we developed a simple device consisting of a PTA-impregnated non-woven material and a low-cost UV lamp that can be used to evaluate the alcohol concentration in saliva and sweat. We further enhanced the practical applicability of this sensor by demonstrating the integration of digital image analysis, multivariate analysis, and mobile camera technology with this sensor. This device can be potentially used in vehicles as a convenient, reusable alcohol sensor for drivers.

1. Introduction

The World Health Organization estimates that diseases and accidents linked to alcohol consumption cause over three million deaths per year. This risk increases in individuals aged 20–39 years, where approximately 13.5% of all deaths can be attributed to alcohol [1]. Alcohol is absorbed directly through the stomach and small intestine, before it passes into the bloodstream where it accumulates, whereas a portion is metabolized by the liver or excreted in the breath, urine, and sweat. Ethanol acts as a central nervous system depressant, and its effects include cognitive, judgment, memory, and motor impairment and sensory dysfunction. When large amounts are consumed in short periods (binge drinking), it may cause vomiting, amnesia, or even death [2].

The standard means of determining alcohol levels in the body is by the direct measurement of the blood alcohol concentration (BAC). BAC is defined as the ratio between the mass of ethanol in a given volume of blood. BAC has been widely adopted as the key parameter in tests to measure alcohol intake. However, BAC cannot be measured *in situ*, as it requires the use of chromatographic methods [3]. Real-time alcohol detection is usually performed with a breathalyzer, which estimates BAC from the concentration of ethanol in the breath. The limitations of this protocol include the high cost of the device, the continuous need for recalibration, and the short lifetime of ethanol in breath [4]. In addition, the use of breathalyzer is typically challenging for people with compromised lung capacity, such as those with asthma and other pulmonary disorders, which restricts them from pumping sufficient amount of breath in the device to allow measurements [5].

As ethanol is dissolved in all body fluids, it can be measured, not only in blood or breath but also in urine, saliva, vitreous fluid, and sweat [5,6]. Saliva and sweat have deserved special attention for use in ethanol measurements because the ethanol levels in these fluids match those of blood after a certain time of ethanol consumption: in saliva: from 20 min of onward from the completion of the drinking (the slope of the relationship: 0.95) [7], and in sweat: 1 h after alcohol consumption (the slope of the relationship: 1.01) [8]. Therefore, in the context of road traffic regulations, both saliva and sweat are good candidates for measuring drivers' blood ethanol

* Corresponding author.
** Corresponding author.
E-mail addresses: vipul.bansal@rmit.edu.au (V. Bansal), josema@urg.es (J.M. Dominguez-Vera).

https://doi.org/10.1016/j.mtchem.2021.100491
2468-5194/

levels. Furthermore, the current illicit drug testing for drivers is based on a saliva swab, and the potential availability of a similar saliva-based test for alcohol can offer a good proposition to regulators and drivers alike.

The concentration of ethanol in human saliva is commonly measured using enzymatic methods. The QED saliva alcohol test, for instance, uses alcohol dehydrogenase and nicotinamide adenine dinucleotide (NAD+) to convert ethanol to acetaldehyde and reduced nicotinamide adenine dinucleotide (NADH) [9]. The NADH is then measured photometrically and correlated to the ethanol concentration in the sample [10]. Alco-Screen is based on two enzymatic reactions: first, alcohol oxidase reacting with the ethanol present in the test sample to produce hydrogen peroxide, which, in a second reaction, oxidizes a color indicator (3,3′,5,5′-tetramethylbenzidine or 2,2′-azino-bis(3-ethylbenzothiazoline-6-sulphonic acid) [11] in the presence of a peroxidase enzyme. Color intensity is related to the concentration of alcohol in the sample.

Sweat has traditionally been an underused resource in non-invasive health monitoring, despite it containing a wealth of physiologically relevant information [12]. Its usage is primarily limited by the fact that it is hard to collect enough sample to quantify analytes, unlike the case of urine or saliva [13]. Two strategies have been developed to overcome this limitation: (1) the use of sweat patches that collect larger volume of sweat, which can later be desorbed and analyzed by gas chromatography [14]; and (2) induced sweat production through physical exercise or pilocarpine iontophoresis (local chemical stimulation of the sweat glands) [15]. Once sweat has been extracted, the ethanol content can be potentially determined by different techniques depending on whether the measurement is *in situ* or it uses enzymatic reactions similar to that in case of saliva [16] or in a laboratory [17].

Polyoxometalates (POMs) have received widespread attention because of their intriguing photoredox chemistry. A particularly interesting property of POMs is photoelectrochromism, that is, their ability to be reduced from a nearly colorless state to a colored form in the presence of an electron (e^-) donor under ultraviolet (UV) light. The reduced POMs, commonly known as 'heteropoly blues', present a characteristic deep blue color, which is visible to the naked eye, even at low concentrations, because of their high extinction coefficients [18–20].

In the present study, we propose a new colorimetric method to measure the ethanol concentration in sweat and saliva using phosphotungstic acid (PTA). Notably, unlike other colorimetric methods, the proposed sensor does not use enzymes, which offers the potential to overcome challenges of high assay costs and enzymatic instability under ambient conditions. PTA, a multiredox-active photoelectrochromic POM molecule, is reduced to an intense blue color by ethanol in the presence of UV light, allowing quantitative detection of ethanol. The subsequent spontaneous oxidation of reduced PTA in air offers a unique feature of reusability to these sensors. Using this concept, we have developed a sensor device based on a PTA-impregnated non-woven material and an inexpensive UV lamp, which in combination with the strengths of mobile camera image capturing and multivariate analysis offers a powerful platform for non-invasive detection of ethanol in body fluids (Fig. 1).

2. Materials and methods

2.1. Reagents and instruments

PTA hydrate ($H_3[P(W_3O_{10})_4]\cdot xH_2O$), phosphomolybdic acid hydrate ($H_3[P(Mo_3O_{10})_4]\cdot xH_2O$), and artificial saliva and sweat constituents were purchased from Sigma–Aldrich. PMO ($Na_6[P_2Mo^{VI}_{18}O_{62}]$) was synthesized as previously reported [21]. Ethanol and acetaldehyde standards were prepared from medicinal ethanol (96%) and synthesis grade acetaldehyde (>99%), respectively, both purchased from Sigma–Aldrich. Reagents were weighted using a BOECO Balance BAS 31 plus (d = 0.1 mg).

The UV light source was a Jiadi 36 Watt Nail Gel Curing UV lamp, consisting of four 9-Watt halogen tubes with λ_{max} at 365 nm (UVA). Headspace gas chromatography (HS-GC) analysis was carried out using a 7890A Agilent (USA) gas chromatographer coupled to a mass spectrometer triple quadrupole Quattro microGC from Waters (USA). UV–visible absorbance spectra of solutions were recorded in a 96-well plate format using a Nanoquant Infinite M200 Pro multilabel plate reader.

2.2. Artificial sweat and saliva formulations

To simulate human sweat and saliva, we used simplified formulations containing the most relevant electroactive species [22,23]. We prepared 100 mL of each fluid by dissolving solutes in distilled and deionized water at the following concentrations:

2 × artificial sweat: 100 mM sodium chloride (NaCl), 5 mM potassium chloride (KCl), 2.5 mM sodium sulfate (Na_2SO_4), 9 mM ammonium chloride (NH_4Cl), 4 mM urea ($CO(NH_2)_2$), 40 mM lactic acid ($CH_3CH(OH)COOH$), 0.24 mM glucose ($C_6H_{12}O_6$), and 0.06 mM ascorbic acid ($C_6H_8O_6$)

2 × artificial saliva: 20 mM sodium chloride (NaCl), 30 mM potassium chloride (KCl), 7 mM potassium phosphate monobasic (KH_2PO_4), 3 mM potassium phosphate dibasic (K_2HPO_4), 4 mM ammonium chloride (NH_4Cl), 2 mM urea ($CO(NH_2)_2$), 2 mM calcium chloride ($CaCl_2$), 0.4 mM magnesium chloride ($MgCl_2$), 3 mM lactic acid ($CH_3CH(OH)COOH$), and 0.25 mM uric acid ($C_5H_4N_4O_3$).

2.3. POMs reduction by ethanol

Three POMs were tested: phosphomolybdic acid (PMA), PTA, and PMO. Aqueous solutions of POMs at 0.1, 1, 5, and 10 mM were exposed to different ethanol concentrations. Even after 1 h, POM reduction was not observed (t = 0). These samples were then irradiated under UV light for 10 min (t = 10 min).

2.4. UV light–induced and ethanol-induced reduction of PTA

A fixed volume (100 μL) of aqueous PTA solution (10 mM) was independently mixed with 100 μL of aqueous ethanol solutions at different concentrations in a 96-well plate to give final ethanol concentrations of 1, 2.6, 5.4, 10.9, and 21.7 mM and the final PTA concentration of 5 mM. We prepared three controls: a mixture of 100 μL of PTA solution and 100 μL of H_2O served as the PTA control; a mixture of 100 μL of PTA solution and 100 μL of artificial saliva was used as the saliva control; and finally, a mixture of 100 μL of PTA solution and 100 μL of artificial sweat served as the sweat control.

To test ethanol concentrations in saliva and sweat samples, ethanol was first diluted (1/100) in artificial saliva or sweat. Then 100 μL of this ethanol in artificial saliva or sweat solutions were independently mixed with 100 μL of an aqueous PTA solution (10 mM), obtaining final ethanol concentrations of 1, 2.6, 5.4, 10.9, and 21.7 mM. The plate was then sealed with an adhesive sealer to prevent potential evaporation during UV light exposure. The plate was exposed to UVA light (365 nm) for 30 min, and the absorbance at 745 nm was recorded using a multilabel plate reader. The tests were performed in triplicates, and the average absorbance at 745 nm was plotted along with standard deviations.

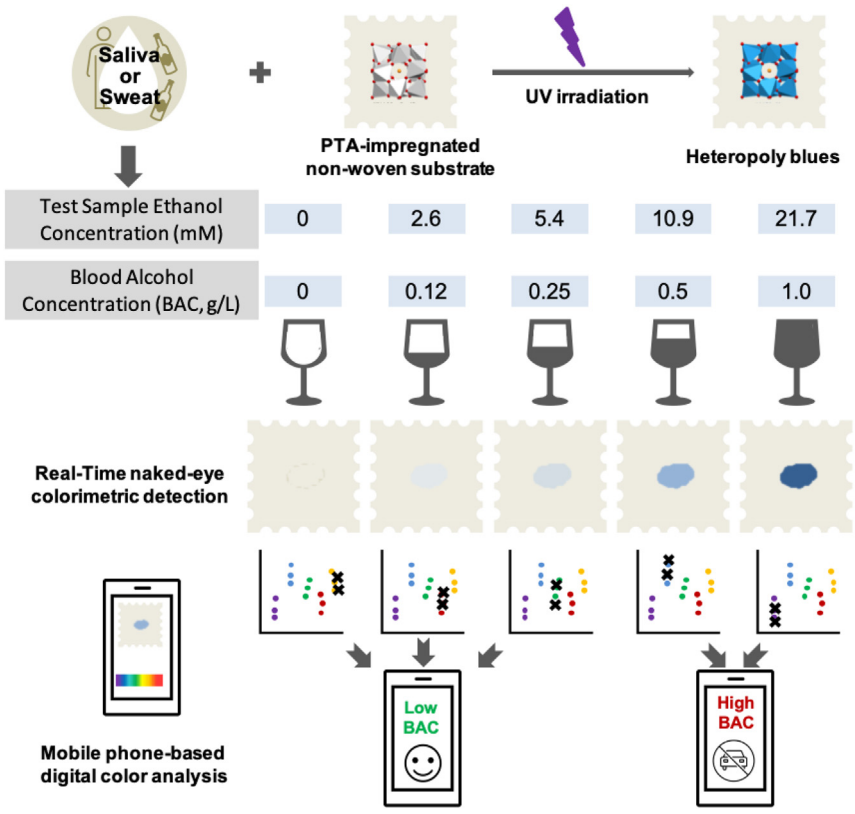

Fig. 1. Schematic of the developed sensor for determining EtOH concentration in sweat and saliva. The method is based on a PTA-impregnated non-woven material, an inexpensive UV lamp and either naked-eye colorimetric detection or mobile phone–based digital color analysis.

2.5. Headspace gas chromatography

We used standards of acetaldehyde and acetaldehyde + ethanol to compare with the three different samples prepared for the HS-GC analysis: (1) PTA-EtOH non-irradiated with UV light, (2) PTA-EtOH irradiated with UV light for 30 min, and (3) PTA-EtOH irradiated with UV light for 210 min. PTA and EtOH concentrations were 5 mM in all cases. Samples were gradually injected into the chromatography column just after been irradiated to avoid reoxidation by air, with the exception of (3) that was injected 24 h after UV light exposure. Vials were maintained at room temperature until insertion into the autosampler, at which time, they were heated to equilibrium at 70 °C for 10 min with an agitation of 500 rpm. A 0.5 mL of headspace sample was injected into the column (capillary column VOCOL from Supelco, USA) with the injector and transfer line both maintained at 220°C. The GC conditions were as follows: column temperature began at 40°C, was held for 2 min, then increased to 200°C at a rate of 8°C/min for a total of 20 min. The GC was operated with a 10:1 split ratio with a 7 mL/min continuous column flow rate using helium as a carrier gas. The MS was operated in electron impact ionization (EI+) mode at 70 eV. The full scan was 20–250 Da, and the source temperature was 220°C.

2.6. PTA reduction–oxidation cycles

These experiments were performed both in solution and on the surface of non-woven substrates. (1) Solution: 1 mL of aqueous PTA solution (10 mM) was mixed with 1 mL of aqueous ethanol solution (21.8 mM) in a 10 mL glass vial with butyl septa to give a final ethanol concentration of 10.9 mM and a final PTA concentration of 5 mM. The sample was exposed to UVA light (365 nm) for 10 min and then left at room temperature for 60 min until they lost the blue color. This cycle was repeated up to 15 times, and blue color development on UV exposure was still repeatedly observed. (2) Non-woven substrate material: A fixed volume (25 μL) of aqueous PTA solution (5 mM) was placed over non-woven substrate material pieces of 15 × 15 mm and dried overnight at 37°C. Once the water in the drop of PTA was totally dried, a solid (PTA) appeared deposited on the surface of the non-woven material. Subsequently, a 10.9 mM EtOH solution was prepared in water, and 25 μL of this diluted ethanol solution was placed over the PTA-embedded non-woven substrate material. The sample over the non-woven substrate material was exposed to UVA light (365 nm) for 10 min. Pictures of the substrates were taken after each UV light irradiation time with a Samsung SM-A920F mobile phone camera, and blue color was followed by the naked eye. The blue drop was left at room temperature to lose blue color and to allow EtOH solution evaporation (around 45 min). Once dried, PTA was left embedded over non-woven substrate material for reuse, and a new 25 μL aliquot of the diluted ethanol solution was added. The cycle was repeated three times, and blue color after the exposure to UV light was still repeatedly observed.

2.7. UV light–induced and ethanol-induced reduction of PTA over non-woven substrate material and linear discriminant analysis

A fixed volume (100 μL) of aqueous PTA solution (5 mM) was placed over several non-woven substrate material pieces of 15 × 15 mm and dried overnight at 37°C. Ethanol was first diluted (1/100) in artificial saliva or sweat. Then, 100 μL of these solutions containing 1, 2.6, 5.4, 10.9, and 21.7 mM ethanol were

independently placed on non-woven substrates over dried PTA. Finally, the samples over the non-woven substrate material pieces were exposed to UVA light (365 nm) for 10 min. Pictures of the substrates were taken after each UV light irradiation event with a Samsung SM-A920F mobile phone camera, and blue color evolution was followed by naked eye. Each test was performed six times. The red, green, and blue (RGB) colors from each sample were picked from a fixed area containing an average of 12 points. Three separate regions were chosen on a single image to generate the RGB matrix where the RGB were displayed as Generic RGB colors. The RGB values of the color images were then tabulated and analyzed by linear discriminant analysis (LDA) to generate independent clusters using the LDA score plots. LDA was performed using OriginPro software. The training set was created through replicate measurement of different ethanol concentrations to create a matrix of six (replicates) × five (concentrations) × three (RGB channels). All raw data were subjected to LDA to differentiate the change in color against ethanol concentration. This was used as the training matrix. The same treatment was applied to another set of data to evaluate the unknown ethanol concentration in the test samples.

3. Results and discussion

POMs are photoelectrochromic molecules, and their reduction to a blue product requires two components, an electron donor and an appropriate photoexcitation source, typically the UV light [24–26]. POMs can, therefore, be used as sensors of UV radiation doses in the presence of a fixed concentration of an appropriate electron donor or as sensors of reducing analytes at a fixed UV dosage. In this sense, we have recently reported that PMA can differentiate between UVA, UVB, and UVC radiation in the presence of lactic acid as an electron donor [18].

A large variety of POMs with a combination of different transition metals (Mo, W, V, Nb, and Ta) and heteroatoms (P, Si, and Al) in their structure are commercially accessible [27–29]. Each of these POMs displays a unique reducibility characteristic for the transition metal embedded in the structure. This implies that by using an appropriate POM molecule and UV light, different electron donors can be potentially detected. In the present work, we use ethanol's capacity to reduce PTA in the presence of UV radiation as a model system to detect alcohol in simulated sweat and saliva formulations. To the best of the authors' knowledge, this is the first time that the application of a POM for colorimetric detection of ethanol is demonstrated.

PTA was determined as the best candidate for alcohol detection from a group of three POMs, including PMA ($[PMo^{VI}_{12}O_{40}]^{3-}$), PMO ($[P_2Mo^{VI}_{18}O_{62}]^{6-}$), and PTA ($[PW^{VI}_{12}O_{40}]^{3-}$) investigated in our current study. Although the aqueous solutions of three POMs are almost colorless (PTA) or with a yellowish tinge (PMO and PMA), their reduced forms are intense blue with broad absorption bands in the UV–vis regions centered around 700–800 nm. First, to establish the proof-of-the-concept, we exposed aqueous solutions containing different concentrations of the three POMs to increasing ethanol concentrations at room temperature. None of the three POMs were reduced directly by ethanol, even at high POM and/or ethanol concentrations (Fig. 2).

We then repeated the previous experiments under UV radiation. As shown in Fig. 2, PTA was reduced after 10 min of UV radiation, even at low ethanol concentrations. The color change was visible to the naked eye at PTA concentrations of 5–10 mM. Interestingly, the blue intensity increased with an increase in the ethanol concentration. Although molybdate-based POMs are generally more effective redox catalysts than tungstates, the observed results are expected as tungstates are more powerful oxidizing agents capable of oxidizing a variety of organic compounds under UV and near-visible radiation [30]. Overall, PTA was clearly the most promising candidate, as it provided the strongest response, that is, an intense blue color visible to the naked eye, thus highlighting the potential of a PTA/UV light system for use as a colorimetric, concentration-sensitive ethanol sensor.

The photoreduction of PTA takes place with the concomitant oxidation of ethanol to acetaldehyde (Fig. 3A) [31]. This was confirmed by (HS-GC), wherein acetaldehyde (MeCHO) and ethanol (EtOH) gave signals at 4.56 min and 5.25 min, respectively, and the positions of those signals were not significantly influenced in the presence of PTA (Fig. 3B). To validate the PTA-induced oxidation of EtOH into MeCHO, UV-exposure time-dependent experiments were performed, which revealed continuously increased production of MeCHO at the expense of EtOH with the increasing UV exposure (Fig. 3C).

Interestingly, when the sample pre-exposed to the UV light was subsequently stored in air for 24 h, no change in the HS-GC profile was observed, suggesting that the reaction abruptly stops once the photoirradiation is discontinued. This strong dependence of PTA-induced EtOH to MeCHO conversion on the presence of UV trigger is quite useful in achieving enhanced sensor stability, as the sensor output will not continue to change once the UV irradiation source is removed. Overall, these investigations support the redox nature of the underlying chemical reaction between PTA and ethanol and its good potential for EtOH sensor development.

An additional advantage of using PTA as an alcohol sensor relies on the fact that its reduced form can spontaneously reoxidize to a colorless form in the air. In this context, PTA acts as a catalyst that can convert to its original form after performing the redox reaction mentioned previously. This oxidation of reduced PTA to its native form solely relies on ambient O_2 without affecting the relative EtOH: MeCHO proportions in the reaction, as evident from the HS-GC data (compare blue and red curves in Fig. 3C). Thus, PTA-based sensors have a good potential to be reused for multiple cycles, as in each cycle, fresh EtOH available to PTA will oxidize to MeCHO on UV exposure without exhausting the catalytic efficiency of PTA [24–26]. In fact, these redox cycles are also the basis of the photocatalytic activity of tungsten-based POMs (e.g. PTA) [28]. In contrast, it is quite hard to reoxidize the reduced forms of molybdenum-based POMs (e.g. PMA and PMO), making PTA a unique molecule for EtOH sensing.

To validate their reusability, once PTA was reduced by ethanol under UV radiation, we exposed the blue sample to air. The blue color completely disappeared after 60 min, returning to the initial colorless PTA. Interestingly, when the sample was exposed to the UV irradiation, it turned blue again. In fact, we could repeat the oxidized–colorless/reduced–blue PTA cycle at least 15 times (Supplementary Information, Fig. S1). The sensor reusability is commonly not achieved with colorimetric sensors, making this property of PTA of paramount importance, as it can be exploited to develop reusable ethanol sensor.

In subsequent experiments, we tested the ability of PTA to detect ethanol in simulant human body fluids, such as sweat and saliva. We first analyzed if the test based on PTA and UV irradiation showed any non-specific cross-reactivity with these simulant body fluids (i.e. color production without ethanol). In this experiment, we added PTA (5 mM) to simulant sweat and saliva, spiked with the highest potential biological concentration of other electroactive species, that is, glucose, lactic acid, ascorbic acid, and uric acid that are known to be generally present in these body fluids [12]. As found in Fig. 4B, in these conditions,

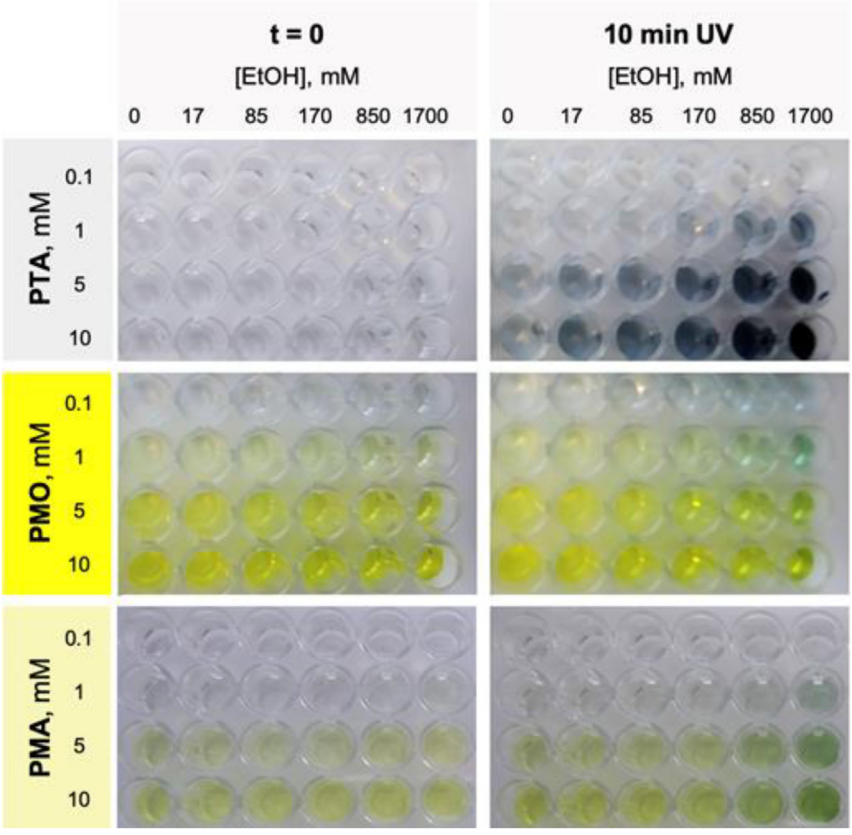

Fig. 2. Ethanol-induced POM (PTA, PMO, and PMA) reduction in the absence or presence of UV light (10 min).

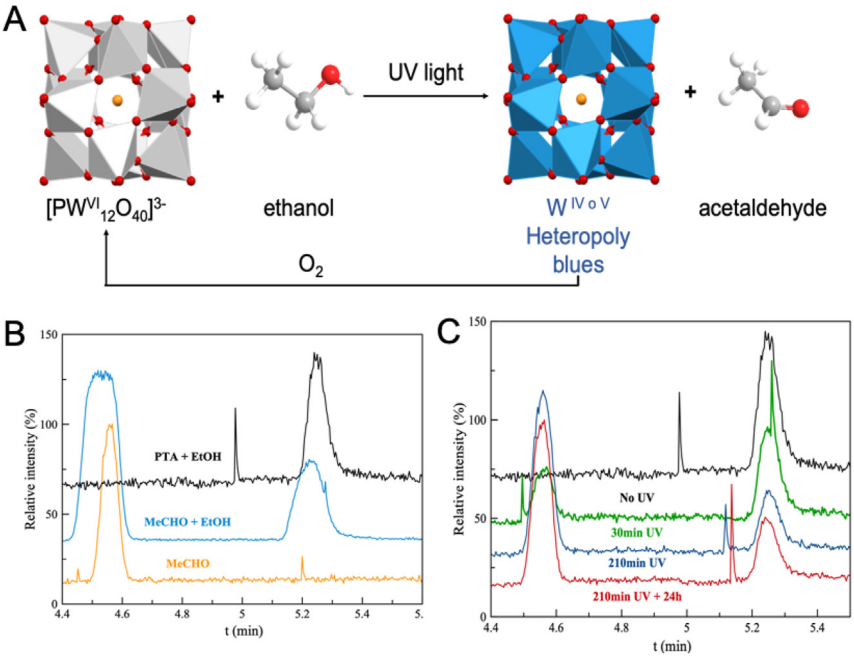

Fig. 3. (A) PTA/ethanol photo-redox cycle. PTA structure was obtained from Crystallography Open Database (COD, 9016537) [32]. The figure was created using Mercury software. (B) HS-GC retention time (t_R) and peak identification: acetaldehyde (4.56 min) and ethanol (5.25 min). (C) HS-GC study of a mixture of PTA and ethanol as a function of UV irradiation time.

hardly any color developed, pointing out that the potentially interfering species in saliva and sweat do not compromise the sensor operation. We subsequently repeated the same experiments with simulated sweat and saliva spiked with different concentrations of ethanol. As evident from Fig. 4, the intensity of the blue color, corresponding to reduced PTA,

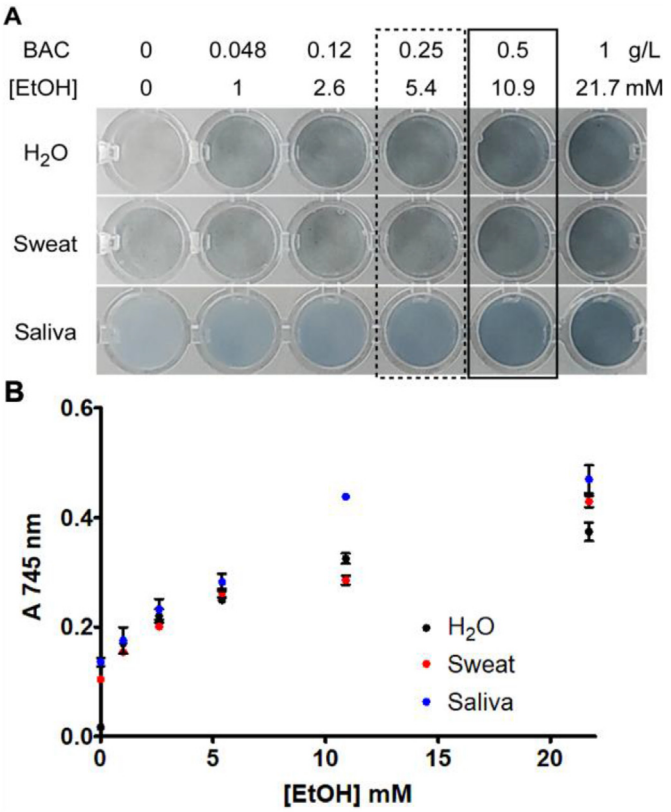

Fig. 4. (A) Photographs of wells with different ethanol concentrations and 5 mM PTA after 30 min of UV radiation. Dashed-line rectangle marks the alcohol rate for novice drivers and black rectangle for standard drivers. (B) Absorbance of the samples at 745 nm after 30 min of UV radiation.

increased with ethanol concentration, becoming especially intense at 5.4 and 10.9 mM ethanol. These ethanol concentrations match BACs of 0.25 and 0.5 g of ethanol in 1 L of blood, which are the maximum permissible alcohol concentrations for novice and standard drivers, respectively, in most countries [33].

Once the ability of PTA to test the permissible alcohol concentrations for drivers was established, we set up a simple device for practical applications by optimizing the UV light exposure time and by embedding PTA in a non-woven substrate material. For this purpose, a fixed amount of PTA solution (5 mM) was drop-casted and dried over non-woven substrates, followed by exposure to simulated sweat and saliva samples containing different ethanol concentrations. After UV irradiation for 10 min, we obtained similar results to those in solution, that is, the intensity of the blue color increased with increasing ethanol concentration (Fig. 5A). However, the limited ability of human eye to detect subtle changes in color intensities may restrict the ability of this sensor to qualitative or, at the best, semiquantitative analysis. To further expand the practical applicability of the proposed EtOH sensor for quantitative detection of EtOH in body fluids, we used digital color analysis of the images captured by a mobile camera. The use of digital analysis has already shown its potential to quantify colorimetric sensor data [34–37] with significant progress already made in high-resolution imaging and low power computing technologies. Further, the underlying algorithms for digital analysis can be easily integrated with existing digital and mobile cameras without requiring significantly new hardware components. The RGB color model is one of the simplest tools that can be used for digital analysis, as an image's color is a combination of these three components in different proportions [36]. The RGB analysis can then either be combined with discriminant analysis or red chromatic shift analysis to gain critical insights into the sensor data, including analyte quantification [34,35,37]. For instance, discriminant analysis of the RGB values has previously allowed the development of a simple tool for solvent identification [34,35]. We adopted a similar approach, wherein we combined the RGB values of the color generated by the sensor with a multivariate discriminant analysis [34,35,38,39] to develop an efficient tool for confidently quantifying ethanol concentrations in simulated sweat and saliva samples. For this, we first assessed the change in color in each case using a color evaluating program, which allowed conversion of the color image into RGB values (Supplementary Information, Figs. S2 and S3). It is clear that the extent of change in the RGB values increases as a function of increasing ethanol concentration in both simulated sweat (Fig. S2) and saliva (Fig. S3). It is also evident that the UV exposure time plays a critical role in the sensor operation with changes in the RGB values maximized on 10-min UV exposure. Therefore, we used LDA as the multivariate statistical analysis tool of choice on the RGB values obtained after 10 min of UV exposure of the sensors to understand the extent of color change under different experimental conditions. LDA allowed quantitative differentiation of the RGB values of sensors on its exposure to each of the tested ethanol concentration (Fig. 5B and C). For instance, the analysis of the RGB values obtained from different concentrations of ethanol in sweat generated three canonical factors where two of the factors were the most significant. The two-dimensional canonical score plot of the two dominant factors showed six independent clusters, each corresponding to different ethanol concentrations used in the present study (Fig. 5B). Although there was no overlap between the clusters, clusters obtained at lower concentrations were close to each other to some extent. It is important to note that the distance between the clusters correlates well with the degree of the color response obtained at different concentrations of ethanol in sweat. Considering that LDA was able to distinguish the different ethanol concentrations, we used this set of data as the training set. We then validated the ability of the RGB-LDA analysis to differentiate among ethanol concentrations in sweat by determining the ethanol concentration in unknown samples (test set). The system could identify the ethanol concentration in the test samples with 100% accuracy. We then extended this approach to assess the photographs of simulated saliva samples on the sensor surface. As seen from the respective canonical plot in Fig. 5C, RGB-LDA could discern different concentrations of ethanol with high resolution, such that clusters corresponding to each ethanol concentration appear independent of each other. Based on this RGB-LDA analysis, we can infer that the proposed sensor offers a limit of detection of 1 mM ethanol in body fluids. Similar to that in the case of sweat, the system could identify the ethanol concentration in the unknown test samples with 100% accuracy. However, significantly better resolution of clusters in saliva samples than in sweat suggests that the precision of the proposed sensor for detecting different concentrations of ethanol is likely to be significantly higher when saliva is used as a choice of body fluid.

Finally, we checked the reusability potential of our ethanol sensing device. For that, a drop of PTA (5 mM) was drop-casted and dried over non-woven substrates, followed by exposure to 10.9 mM of EtOH (0.5 g/L BAC). After UV radiation (10 min), a blue color developed. Once air-dried, we repeated the same cycle twice more, resulting in the reappearance of blue color (Fig. 5D). This suggests that the proposed ethanol sensing device is reusable.

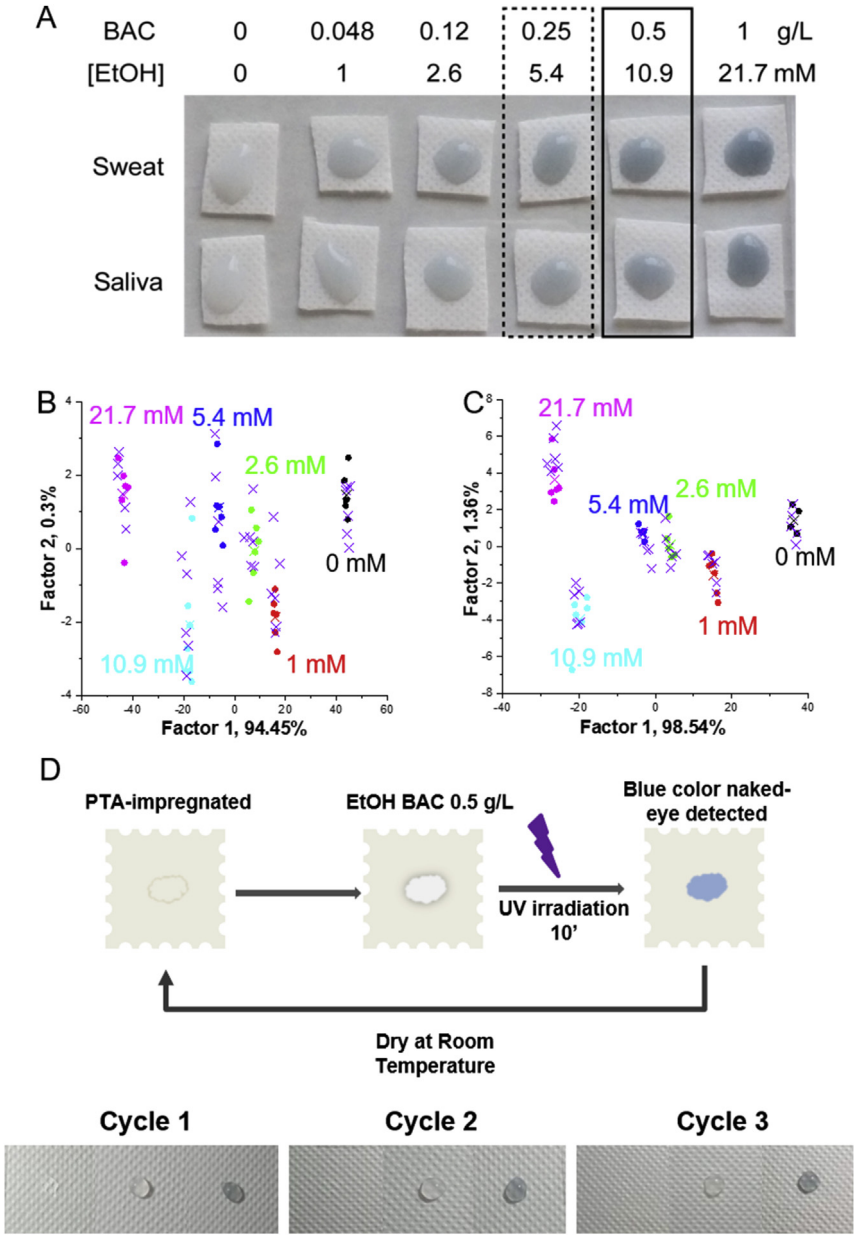

Fig. 5. (A) Representative photographs showing changes in the colors of sweat and saliva samples containing different ethanol concentrations on the surface of non-woven substrate sensors preconditioned with 5 mM PTA after 10 min of UV radiation. Dashed-line rectangle marks the alcohol rate for novice drivers, and solid-line rectangle marks the alcohol rate for standard drivers. (B and C) Canonical score plot for the RGB values obtained from LDA for different ethanol concentrations in (B) sweat and (C) saliva after 10 min of UV exposure. The solid spheres (•) show clustering of data for different ethanol concentrations as obtained from LDA analysis of the training set, whereas the crosses (×) show the ability of the chosen algorithm to confidently detect the concentration of ethanol in unknown samples (test set). (D) Sensor reusability study tested over a non-woven substrate using 10.9 mM of EtOH (0.5 g/L) and 10 min of UV radiation. In each cycle, the first photograph corresponds to a PTA-impregnated substrate, whereas the second and third photographs represent the EtOH solutions before and after UV exposure, respectively.

4. Conclusion

We have developed a new strategy for determining blood alcohol content by measuring ethanol concentration in saliva and sweat. This system is based on the use of colorless PTA as a photoelectrochromic agent and a low-cost UV lamp. The alcohol concentration correlated with the intensity of the blue color produced by reduced PTA, allowing quantitative colorimetric detection of ethanol. Furthermore, after exposure to ambient air, the reduced PTA was oxidized back to its original colorless form, providing a unique potential for the reusability of the ethanol sensor. Based on these properties, we developed a simple device, consisting of a PTA-impregnated non-woven substrate material and a low-cost UV lamp, which can be used to evaluate the alcohol concentration in saliva and sweat. By incorporating digital color analysis with the colorimetric sensor system, we showed the potential applicability of the system to be used on site without any need for sophisticated equipment. This simple sensor device that works with higher precision on saliva than in sweat can be used in vehicles as a convenient, reusable alcohol sensor for drivers.

Data availability

The raw data required to reproduce these findings cannot be shared at this time because of technical (large sizes of mobile camera photos). The processed data are reflected from the figures provided in main article and the supplementary information.

Authors' contributions

M.S., A.G., L.S., and W.Z. performed the wet experiments. R.R. performed the image analyses. V.B. and J.M.D. conceptualized the idea and wrote the final version of the published article with contributions from all the authors.

Declaration of competing interest

The authors declare that they have no known competing financial interests or personal relationships that could have appeared to influence the work reported in this paper.

Acknowledgments

This work was funded by the Spanish Ministerio de Ciencia, Innovación y Universidades (MICIU) (project FEDER PID2019-111461 GB-I00). A.G. acknowledges Junta de Andalucía for the postdoctoral contract within the PAIDI 2020 program (DOC_00791). L.S. acknowledges the Spanish MICIU for the predoctoral contract within the FPU program (FPU16/01360). The authors also thank the 'Unidad de Excelencia Química aplicada a Biomedicina y Medioambiente' (UGR) for funding support. V.B. acknowledges Ian Potter Foundation for establishing Sir Ian Potter NanoBioSensing Facility at RMIT University.

Appendix A. Supplementary data

Supplementary data to this article can be found online at https://doi.org/10.1016/j.mtchem.2021.100491.

References

[1] J.H. Hammer, M.C. Parent, D.A. Spiker, Global Status Report on Alcohol and Health 2018, World Health Organization, 2019.
[2] A. Papalimperi, S. Athanaselis, A. Mina, I. Papoutsis, C. Spiliopoulou, S. Papadodima, Incidence of fatalities of road traffic accidents associated with alcohol consumption and the use of psychoactive drugs: a 7-year survey (2011-2017), Exp. Ther. Med. 18 (2019) 2299–2306.
[3] M.E. Hair, R. Gerkman, A.I. Mathis, L. Halámková, J. Halámek, Noninvasive concept for optical ethanol sensing on the skin surface with camera-based quantification, Anal. Chem. 91 (2019) 15860–15865.
[4] E. Bihar, Y. Deng, T. Miyake, M. Saadaoui, G.G. Malliaras, M. Rolandi, A disposable paper breathalyzer with an alcohol sensing organic electrochemical transistor, Sci. Rep. 6 (2016) 2–7.
[5] A.W. Jones, Physiological aspects of breath-alcohol measurement, Alcohol, Drugs Driv. 6 (1990) 1–25.
[6] R. Swift, Direct measurement of alcohol and its metabolites, Addiction 98 (2003) 73–80.
[7] K.E.L. McColl, B. Whiting, M.R. Moore, A. Goldberg, Correlation of ethanol concentrations in blood and saliva, Clin. Sci. 56 (1979) 283–286.
[8] M.J. Buono, Sweat ethanol concentrations are highly correlated with co-existing blood values in humans, Exp. Physiol. 84 (1999) 401–404.
[9] A.S. Santos, R.S. Freire, L.T. Kubota, Highly stable amperometric biosensor for ethanol based on Meldola's blue adsorbed on silica gel modified with niobium oxide, J. Electroanal. Chem. 547 (2003) 135–142.
[10] T.A. Christopher, J.A. Zeccardi, Evaluation of the ethanol in saliva alcohol test : a new, rapid, accurate device for measuring from the division of emergency, Ann. Emerg. Med. 21 (1992) 1135–1137.
[11] Y. Jung, J. Kim, O. Awofeso, H. Kim, F. Regnier, E. Bae, Smartphone-based colorimetric analysis for detection of saliva alcohol concentration, Appl. Opt. 54 (2015) 9183–9189.
[12] M. Bariya, H. Yin, Y. Nyein, A. Javey, Wearable sweat sensors, Nat. Electron. 1 (2018) 160–171.
[13] D.A. Kidwell, J.C. Holland, S. Athanaselis, Testing for drugs of abuse in saliva and sweat, J. Chromatogr. B Biomed. Appl. 713 (1998) 111–135.
[14] M. Phillips, M.H. McAloon, A sweat-patch test for alcohol consumption: evaluation in continuous and episodic drinkers, Alcohol Clin. Exp. Res. 4 (1980) 391–395.
[15] J. Kim, I. Jeerapan, S. Imani, T.N. Cho, A. Bandodkar, S. Cinti, P.P. Mercier, J. Wang, Noninvasive alcohol monitoring using a wearable tattoo-based iontophoretic-biosensing system, ACS Sens. 1 (2016) 1011–1019.
[16] M. Gamella, S. Campuzano, J. Manso, G.G. de Rivera, F. López-Colino, A.J. Reviejo, J.M. Pingarrón, A novel non-invasive electrochemical biosensing device for in situ determination of the alcohol content in blood by monitoring ethanol in sweat, Anal. Chim. Acta 806 (2014) 1–7.
[17] C. Schummer, B.M.R. Appenzeller, R. Wennig, Quantitative determination of ethyl glucuronide in sweat, Ther. Drug Monit. 30 (2008) 536–539.
[18] W. Zou, A. González, D. Jampaiah, R. Ramanathan, M. Taha, S. Walia, S. Sriram, M. Bhaskaran, J.M. Dominguez-Vera, V. Bansal, Skin color-specific and spectrally-selective naked-eye dosimetry of UVA, B and C radiations, Nat. Commun. 9 (2018) 1–10.
[19] A. González, N. Gálvez, M. Clemente-León, J.M. Dominguez-Vera, Electrochromic polyoxometalate material as a sensor of bacterial activity, Chem. Commun. 51 (2015) 10119–10122.
[20] N. Saenz, M. Sánchez, N. Gálvez, F. Carmona, P. Arosio, J.M. Dominguez-Vera, Insights on the (auto)photocatalysis of ferritin, Inorg. Chem. 55 (2016) 6047–6050.
[21] R. Strandberg, H. Hjersing, A. Kjekshus, A.F. Andresen, J.T. Southern, K. Edlund, M. Eliasen, C. Herskind, T. Laursen, P.M. Pedersen, Multicomponent polyanions. 12. The crystal structure of $Na_6Mo_{18}P_2O_{62}(H_2O)_{24}$, a compound containing sodium coordinated 18-molybdodiphoshate anions, Acta Chem. Scand. 29 (1975) 350–358.
[22] A.B. Stefaniak, C.J. Harvey, Dissolution of materials in artificial skin surface film liquids, Toxicol. Vitro 20 (2006) 1265–1283.
[23] L. Wong, C.H. Sissions, A comparison of human dental plaque microcosm biofilms grown in an undefined medium and a chemically defined artificial saliva, Arch. Oral Biol. 46 (2001) 477–486.
[24] A. Pearson, S.K. Bhargava, V. Bansal, UV-switchable polyoxometalate sandwiched between TiO2 and metal nanoparticles for enhanced visible and solar light photocatalysis, Langmuir 27 (2011) 9245–9252.
[25] A. Pearson, H. Zheng, K. Kalantar-Zadeh, S.K. Bhargava, V. Bansal, Decoration of TiO_2 nanotubes with metal nanoparticles using polyoxometalate as a UV-switchable reducing agent for enhanced visible and solar light photocatalysis, Langmuir 28 (2012) 14470–14475.
[26] A. Pearson, S. Bhosale, S.K. Bhargava, V. Bansal, Combining the UV-switchability of Keggin ions with a galvanic replacement process to fabricate TiO_2-polyoxometalate-bimetal nanocomposites for improved surface enhanced Raman scattering and solar light photocatalysis, ACS Appl. Mater. Interfaces 5 (2013) 7007–7013.
[27] B. Artetxe, S. Reinoso, L. San Felices, P. Vitoria, A. Pache, J. Martín-Caballero, J.M. Gutiérrez-Zorrilla, Functionalization of Krebs -type polyoxometalates with N,O-chelating ligands: a systematic study, Inorg. Chem. 54 (2015) 241–252.
[28] B. Artetxe, S. Reinoso, L. San Felices, L. Lezama, J.M. Gutiérrez-Zorrilla, C. Vicent, F. Haso, T. Liu, New perspectives for old clusters: Anderson-Evans anions as building blocks of large polyoxometalate frameworks in a series of heterometallic 3d- 4f species, Chem. Eur J. 22 (2016) 4616–4625.
[29] J.J. Baldoví, J.M. Clemente-Juan, E. Coronado, Y. Duan, A. Gaita-Ariño, C. Giménez-Saiz, Construction of a general library for the rational design of nanomagnets and spin qubits based on mononuclear f.block complexes. The polyoxometalate case, Inorg. Chem. 53 (2014) 9976–9980.
[30] E. Papaconstantinou, Photochemistry of polyoxometalates of molybdenum and tungsten and/or vanadium, Chem. Soc. Rev. 18 (1989) 1–31.
[31] E. Papaconstantinou, Photocatalytic oxidation of organic compounds using heteropoly electrolytes of molybdenum and tungsten, J. Chem. Soc. Chem. Commun. (1982) 12–13.
[32] J.F. Keggin, The structure and formula of 12-phosphotungstic acid, Proc. Roy. Soc. Lond. 144 (1934) 75–100.
[33] Wikipedia, Drunk driving law by country, (n.d.). ://en.wikipedia.org/wiki/Drunk_driving_law_by_country (accessed May 4, 2020).
[34] S. Pumtang, W. Siripornnoppakhun, M. Sukwattanasinitt, A. Ajavakom, Solvent colorimetric paper-based polydiacetylene sensors from diacetylene lipids, J. Colloid Interface Sci. 364 (2011) 366–372.
[35] T. Eaidkong, R. Mungkarndee, C. Phollookin, G. Tumcharern, M. Sukwattanasinitt, S. Wacharasindhu, Polydiacetylene paper-based colorimetric sensor array for vapor phase detection and identification of volatile organic compounds, J. Mater. Chem. 22 (2012) 5970–5977.
[36] M.J. Kangas, R.M. Burks, J. Atwater, R.M. Lukowicz, P. Williams, A.E. Holmes, Colorimetric sensor arrays for the detection and identification of chemical weapons and explosives, Crit. Rev. Anal. Chem. 47 (2017) 138–153.
[37] M. Weston, R.P. Kuchel, R. Chandrawati, Digital analysis of polydiacetylene quality tags for contactless monitoring of milk, Anal. Chim. Acta 1148 (2021) 238190.
[38] N. Zohora, D. Kumar, M. Yazdani, V.M. Rotello, R. Ramanathan, V. Bansal, Rapid colorimetric detection of mercury using biosynthesized gold nanoparticles, Colloids Surfaces A Physicochem. Eng. Asp. 532 (2017) 451–457.
[39] H. Muhamadali, A. Subaihi, M. Mohammadtaheri, Y. Xu, D.I. Ellis, R. Ramanathan, V. Bansal, R. Goodacre, Rapid, accurate, and comparative differentiation of clinically and industrially relevant microorganisms: via multiple vibrational spectroscopic fingerprinting, Analyst 141 (2016) 5127–5136.